

Polymer Chemistry

Accepted Manuscript

This article can be cited before page numbers have been issued, to do this please use: B. Brati, P. Altenbuchner, T. Heuser and B. Rieger, *Polym. Chem.*, 2025, DOI: 10.1039/D5PY00247H.



This is an Accepted Manuscript, which has been through the Royal Society of Chemistry peer review process and has been accepted for publication.

Accepted Manuscripts are published online shortly after acceptance, before technical editing, formatting and proof reading. Using this free service, authors can make their results available to the community, in citable form, before we publish the edited article. We will replace this Accepted Manuscript with the edited and formatted Advance Article as soon as it is available.

You can find more information about Accepted Manuscripts in the [Information for Authors](#).

Please note that technical editing may introduce minor changes to the text and/or graphics, which may alter content. The journal's standard [Terms & Conditions](#) and the [Ethical guidelines](#) still apply. In no event shall the Royal Society of Chemistry be held responsible for any errors or omissions in this Accepted Manuscript or any consequences arising from the use of any information it contains.

ARTICLE

View Article Online
DOI: 10.1039/D5PY00247H

5-Ethylidene-2-norbornene (ENB) and 5-Vinyl-2-norbornene (VNB) based Alicyclic Polyols for the Synthesis of Polyesters

Brigita Bratić,^a Peter Altenbuchner,^b Thomas Heuser,^b and Bernhard Rieger^{*a}Received 00th January 20xx,
Accepted 00th January 20xx

DOI: 10.1039/x0xx00000x

Amorphous polyesters derived from rigid alicyclic monomers with high glass transition temperatures are of great interest as potential substitute for poly(carbonate)s. Therefore, 5-ethylidene-2-norbornene (ENB) and 5-vinyl-2-norbornene (VNB) were identified as interesting diol monomer precursors to enhance the thermal properties of polyesters. The regioselective synthesis of the corresponding diols from ENB and VNB were optimized and first scale up experiments gave promising results for a potential large scale production of these polyester monomers. Moreover, for proof of concept, an alternative procedure was established to synthesize exclusively *branched* diols. Polymerization experiments were conducted with dimethyl terephthalate (DMT) as model compound to compare the polyesters with commonly used poly(ethylene terephthalate)s. Therefore, a series of polyesters were produced containing *branched* or *linear* or a mixture of both regioisomers, and structure-property relationships were investigated with GPC, TGA and DSC analysis. The T_g values ranged from 75–103 °C, depending on the *branched* and *linear* moieties in the polyester microstructure and their molecular weights. Moreover, isosorbide (IS) was introduced as biobased comonomer, resulting in amorphous copolyesters with promising T_g s ranging from 81 to 97 °C.

Introduction

Polymers, with their versatile properties, became indispensable in today's world since they fulfil a wide range of needs across industries, driving innovation and sustainability efforts. Their adaptability ensures they will remain at the forefront of technological advancements for years to come.^{1–2} The development of new polymer materials is therefore of utmost importance due to the increasing requirements regarding performance and safety.^{1–4} One example for increasing safety standards is the impending worldwide ban of bisphenol-A based polycarbonates (BPA-PC) due to their endocrine disrupting effects and toxicity.^{5–8} A potential candidate for the replacement of such widely used BPA based polymers could be amorphous polyesters, assuring that they exhibit comparable properties such as high heat resistance and clarity to fulfil market requirements. However, in this regard most amorphous polyesters are often limited due to their low glass transition temperature (T_g), which is an important thermomechanical property for their practical application in industry like food packaging materials or coil coating.^{4, 9–10} Amorphous polyesters with high T_g s are thermally stable, enabling them to endure higher temperatures without deformation or structure loss. This stability is required in food packing, where products may

ensures shape and barrier properties of packaging materials.^{10–11}

Moreover, high T_g polyesters exhibit superior barrier properties against gases, moisture and scents, crucial for preserving product freshness and quality.¹² Additionally, their enhanced mechanical properties ensure better protection for packaged products during handling, transportation and storage.³ In applications such as coil coating, where the coating must withstand mechanical stresses and deformation, a high T_g guarantee the maintenance of structural integrity.¹³

An option to improve the thermal properties of polyesters is the incorporation of rigid cyclic structures into the polyester backbone, which has been already demonstrated in the literature. For example, tricyclodecanedimethanol (TCD-DM) was studied by the group of *Fenouillot* resulting in amorphous polyester materials with T_g s ranging from 116 to 163 °C.¹⁴ Among TCD-DM, isosorbide (IS) was studied extensively in the synthesis and modification of polyester materials with varying isosorbide content.^{10, 14–24} Further interesting examples are 2,2,4,4-tetramethyl-1,3-cyclobutanediol (TMCD)^{12, 25–27}, which is known for the production of high-performance Tritan™ (*Eastman*) or spiroglycol (SPG)¹, which is used for the production of Akestra™ (*Perstorp AB*). The substitution of terephthalic acid (TPA) or dimethyl terephthalate (DMT) has been a topic of research in food packaging as well, leading to many examples of dimethyl ester 2,5-furandicarboxylate (DMFD) based polyesters with remarkable thermal and barrier material properties.^{10–11, 28–30} All these polymers exhibit high T_g s and can be even produced from biobased sources.

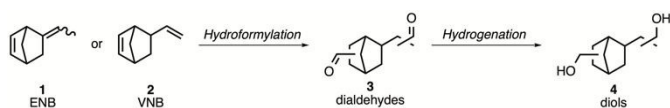
^a Technical University of Munich, WACKER Chair of Macromolecular Chemistry, Department of Chemistry, D-85748 Garching bei München, Germany, E-mail: rieger@tum.de; Tel: +49 (0)89 289 54448

^b Evonik Operations GmbH, Paul-Baumann-Straße 1, D-45772 Marl, Germany, E-Mail: peter.altenbuchner@evonik.com, thomas.heuser@evonik.com

[†]Supplementary information (SI) available: Experimental (monomer synthesis, polymerisation); additional ¹H, ¹³C and DOSY NMR spectra, thermal analysis (TGA and DSC), GPC data. See DOI: 10.1039/x0xx00000x

undergo heating during processing or storage, as high T_g





Scheme 1. Catalytic hydroformylation of ENB (1) or VNB (2) to a mixture of dialdehyde regioisomers (3) followed by hydrogenation to the corresponding diols (4).

Nature provides a rich diversity of diene structures, which are potential precursors for the synthesis of diols, yet their availability for large-scale polymer production is often constrained by factors such as reactivity issues, extraction and high cost.³¹ With our search for new polyesters in mind, we identified 5-ethylidene-2-norbornene (ENB, 1) and 5-vinyl-2-norbornene (VNB, 2) as interesting monomer-precursors, a readily available feedstock from the ethylene-propylene-diene monomer (EPDM) industry, which are produced on a multi-million metric ton per year scale.³² Their bicyclic core not only provides rigidity, the corresponding diols (4) should be accessible via a hydroformylation-reduction sequence (Scheme 1). Our research aims to develop an efficient process, which offers a new pathway to produce cycloaliphatic diols in a cost-effective and scalable manner. Moreover, this development could enable the production of additional downstream products, such as amines, carboxylic acids, and methyl methacrylates. Furthermore, the nature of the *exocyclic* double bonds in ENB (1) and VNB (2) allows control of the regioselectivity (*linear* vs. *branched* diols). Thus, the polyester backbone can be modified and therefore, the properties of the polymer can be finetuned to its respective requirement. In the current study we investigated the influence of the isomer composition of the aforementioned diols on the thermal properties of polyesters.

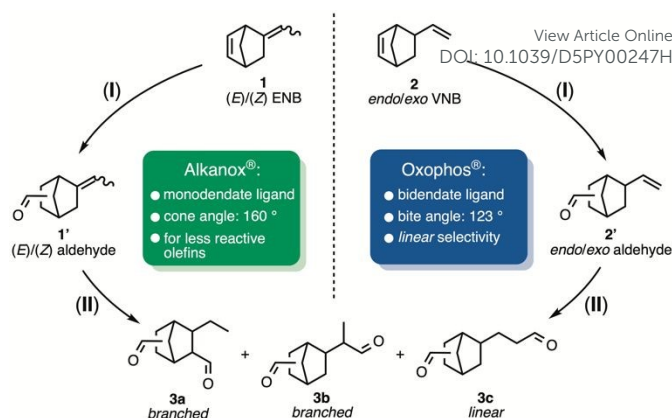
In this context, we conducted an optimization of the hydroformylation reaction and developed modified synthesis strategies for diols 4 (Scheme 1). Our goal was to scale up the production process of compounds 3 and 4 to a multigram scale, aiming to produce amorphous polyesters with promising thermal properties. These polyesters—show potential applications in food packaging and coil coating.

Results and Discussion

Optimizing monomer synthesis for industrial-scale production

While the synthesis of diols from ENB (1) and VNB (2) has been previously described in a patent, the reported conditions required high temperatures and pressures, which are not ideal for large-scale production.³³ Furthermore, the available synthetic procedures and analytical data were limited. Given that diols 4 are excellent candidates for polyester monomers, the reaction sequence was re-evaluated to establish milder conditions that enhance scalability and reduce production cost.

ENB (1) and VNB (2) are commercially available as a mixture of *cis/trans* and/or *endo/exo* diastereomers, and the reactivity of their *endo*- and *exocyclic* double bonds may influence the regioselectivity of their *di*-hydroformylation. Due to the inherent ring strain of the bicyclic structures, hydroformylation



Scheme 2. Possible reaction sequences in *di*-hydroformylation of ENB (1) and VNB (2) using Alkanox® or Oxophos® as ligands.

typically proceeds via an initial reaction at the *endocyclic* double bond (I), followed by the less favoured hydroformylation of the *exocyclic* double bond (II) (Scheme 2). Optimizing reaction conditions – including pressure, temperature, reaction time, and phosphorus ligand selection – was therefore necessary to minimize undesired byproducts. The hydroformylation conditions were screened using bis(1,5-cyclooctadiene)rhodium (I) tetrafluoroborate [Rh(COD)₂]BF₄ as the precatalyst, in conjunction with the regio-directing phosphorus ligands Alkanox® and Oxophos®, which allow milder reaction conditions.^{31, 34–35} Additionally, (S_{ax},S_s)-bobphos^{36–37} was tested, and a full screening of reaction conditions did not improve conversion or regioselectivity. Consequently, due to these limitations and the scope of this study, this approach was not pursued further. For analysis, a combination of nuclear magnetic resonance (NMR) spectroscopy and gas chromatography mass spectrometry (GC MS) was employed due to the formation of multiple isomers, including diastereomers and regioisomers.

Hydroformylation experiments. The hydroformylation of ENB (1) was conducted with Alkanox® as the ligand at temperatures ranging from 40 to 140 °C in 20 °C increments, with an initial reaction time of three hours. The conversion was monitored by

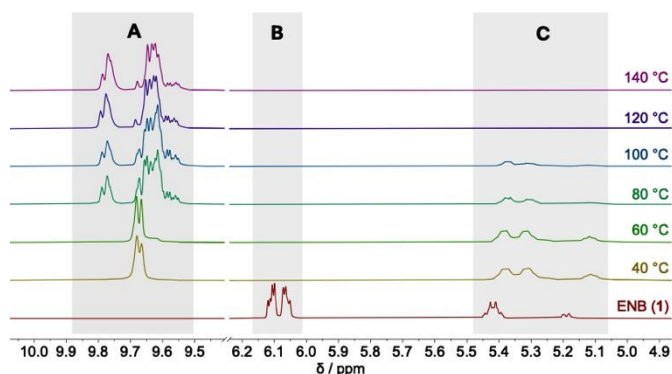


Figure 1. Stacked ¹H NMR spectra from hydroformylation reactions of ENB (1) at different temperatures after three hours using Alkanox® as the ligand; reaction conditions: 0.10 mol% [Rh(COD)₂]BF₄, 0.35 mol% Alkanox®, CO/H₂ = 1/1, 50 bar, 40–140 °C, 3h, (PhMe, 1 M).



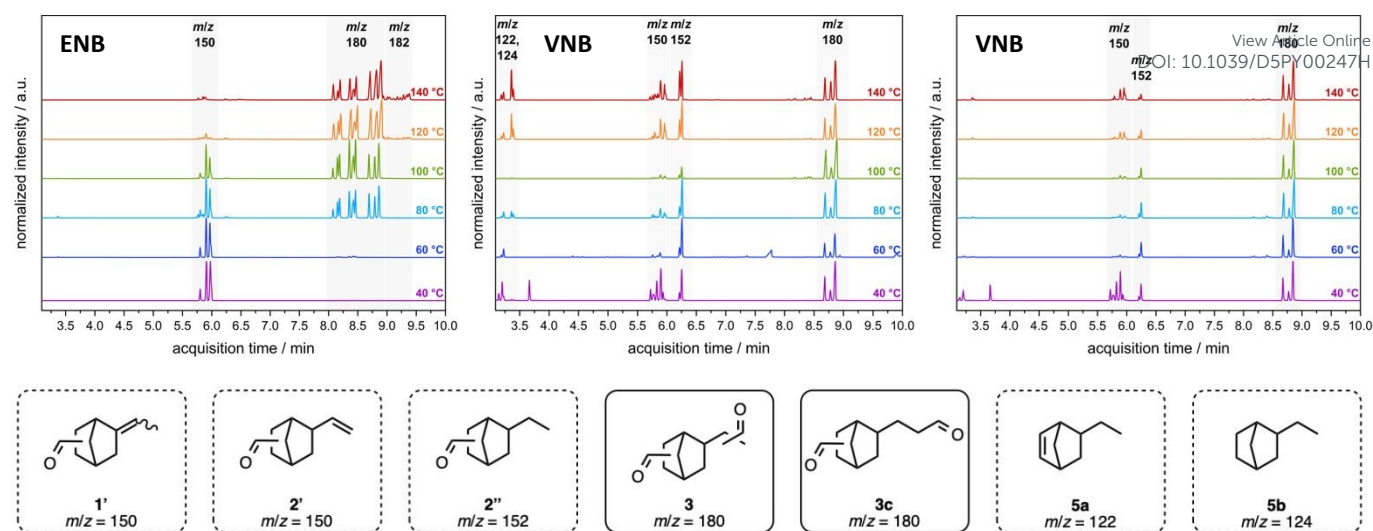


Figure 2. Stacked GC chromatograms from hydroformylation reactions of ENB (1) and VNB (2) at different temperatures after three hours; reaction conditions: (left) 24.96 mmol ENB (1), 0.10 mol% [Rh(COD)₂]BF₄, 0.31 mol% Alkanox®, CO/H₂ = 1/1, 50 bar, 40–140 °C, (PhMe, 1 M). (middle) 24.96 mmol VNB (2), 0.10 mol% [Rh(COD)₂]BF₄, 0.11 mol% Oxophos®, CO/H₂ = 1/1, 50 bar, 40–140 °C, (PhMe, 1 M). (right) 24.96 mmol VNB (2), 0.10 mol% [Rh(COD)₂]BF₄, 0.11 mol% Oxophos®, CO/H₂ = 3/2, 50 bar, 40–140 °C, (PhMe, 1 M). Byproducts: aldehydes 1' (m/z = 150) result from ENB (1) hydroformylation; aldehydes 2' (m/z = 150) and 2'' (m/z = 152) result from VNB (2) hydroformylation; hydrogenated compounds 5a (m/z = 122) and 5b (m/z = 124) emerge as byproducts from VNB (2) hydroformylation with a syngas ratio of CO/H₂ = 1/1.

¹H NMR spectroscopy. The characteristic resonance of the endocyclic double bond were observed at δ_{1H} = 6.10 ppm and δ_{1H} = 6.05 ppm (B), while resonances at δ_{1H} = 5.42 ppm and δ_{1H} = 5.19 ppm (C) correspond to the *cis/trans* exocyclic double bond (Figure 1). At 40 and 60 °C, ENB (1) was fully converted to monoaldehydes 1', which subsequently formed dialdehydes 3 upon increasing the reaction temperature to 80 or 100 °C (A). The gradual shift in exocyclic double bond resonances confirmed the formation of new products, with decreasing intensity at higher temperatures indicating partial conversion of 1' to dialdehydes 3 (C). At 120 and 140 °C full conversion was achieved, and new aldehyde resonances between 9.0 to 10 ppm confirmed the presence of dialdehydes 3 (A).

The gathered information from the proton NMR spectra gave important insights in the reaction sequence of ENB (1) hydroformylation. However, signal overlap impeded further analysis and understanding of the reaction. Consequently, the experiments were also examined with GC MS and additional information could be collected (Figure 2, left). Hydroformylation of ENB (1) at 40 and 60 °C resulted in aldehydes 1' with exclusive mono hydroformylation (m/z = 150). Increasing the temperature to 80 and 100 °C led to the desired dialdehydes 3 (m/z = 180), but with aldehydes 1' not yet fully converted. Full conversion of aldehydes 1' was achieved at 120 and 140 °C, but partial reduction of the desired product was observed as side reaction (m/z = 182). Thus, for initial scale-up the reaction was performed overnight at 100 °C full conversion of 1' without formation of undesired by-products.

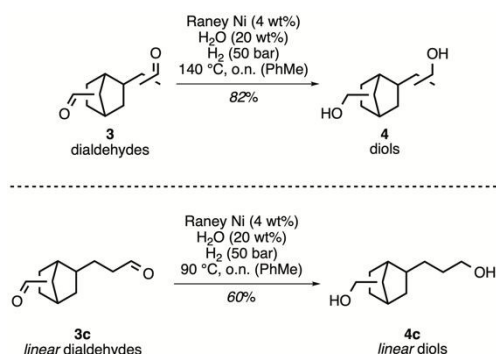
Despite the use of Alkanox® to control regioselectivity in ENB (1) hydroformylation, selectivity challenges remained. To address this, Oxophos® was used in the hydroformylation of VNB (2) to preferentially generate linear dialdehydes 3c.³¹ This approach leveraged VNB's (2) less sterically hindered exocyclic double bond, in combination with the regio-directing effects of Oxophos®, facilitating the selective formation of linear

dialdehydes 3c. Examination of the reaction between 40 and 140 °C using a syngas ratio of CO/H₂ = 1/1 resulted in a mixture of products (Figure 2, middle). Across this temperature range, byproducts 5a (m/z = 122) and 5b (m/z = 124) were detected along with the aldehydes 2' (m/z = 150) and 2'' (m/z = 152). Compared to the reaction of ENB (1) with Alkanox® (Figure 2, left) the number of signals for dialdehydes 3 decreased and could be assigned to linear dialdehydes 3c by ¹H and ¹³C NMR spectroscopy. In an attempt to prevent reduction as a side reaction, the syngas ratio CO/H₂ was adjusted from 1/1 to 3/2 (Figure 2, right).^{35, 38} At 40 °C, aldehydes 2' and byproduct 2'' were observed along with the desired linear dialdehydes 3c, but the formation of 2' and 2'' was significantly decreased at higher temperatures (60–100 °C). At 120 and 140 °C, the signal intensities of 2' and 2'' increased again, presumably due to decomposition of the ligand Oxophos®.³⁹ Therefore, the best result was obtained at 100 °C and CO/H₂ = 3/2, and these conditions were used for initial scale-up.

To explore *iso*-selective hydroformylation for branched dialdehydes 3a+3b, the chiral ligand (*S*_{ax},*S*_S)-bobphos was tested with ENB (1). Reactions were conducted at 40–80 °C (CO/H₂ = 1/1) for 24h, and analysed by GC MS. At 40 °C, mainly aldehydes 1' were formed. At 60 °C, a mixture of branched dialdehydes 3a+3b and aldehydes 1' was detected. At 80 °C, selectivity decreased due to formation of a mixture of 3 and undesired reduction products. Further screening of catalyst and ligand loading at 60 °C did not improve conversion or regioselectivity and consequently, this approach was not pursued further.

The hydroformylation reactions were optimized for scalability by adjusting temperature and pressure in Rh-catalysed reactions of ENB (1) and VNB (2). Initial scale-up was performed in a 2 L batch reactor with a batch size of 416 mmol. Purification via vacuum distillation yielded colourless liquids with 76% yield for dialdehydes 3 and 40% yield for linear





Scheme 3. Optimized hydrogenation strategy for scale up synthesis of diols **4** and linear diols **4c**.

dialdehydes **3c**. Despite high conversions, yield losses were observed during vacuum distillation, likely due to viscosity increases in the residue. Gradual temperature increases were applied to mitigate yield loss, but aldehyde side reactions (e.g. dehydrogenation or decomposition) may occur due to the low decomposition temperature of dialdehydes **3** ($T_d = 107$ °C, see SI†). Moreover, stability studies of dialdehydes **3** revealed acetalization as potential side reaction, which was identified using FT-IR and ESI-MS (see SI†, Figure S2 and Table S1).

Hydrogenation experiments. The hydrogenation of dialdehydes **3** and linear dialdehydes **3c** was investigated using two different approaches: (a) hydrogenation of the crude product mixture, and (b) hydrogenation of the previously purified dialdehydes **3** and linear dialdehydes **3c**.⁴⁰

Initial hydrogenation attempts of dialdehydes **3** were conducted following strategy (a) on a 24.96 mmol scale, using 2 wt% Raney nickel and 10 wt% H₂O. The addition of water could significantly improve the yield, thus, water was incorporated into the crude reaction mixture of **3** post-hydroformylation.⁴⁰ The reactions were evaluated across a temperature range of 25 to 140 °C at 50 bar H₂, and the desired products were subsequently isolated via vacuum distillation (Table 1). Reaction progress was meticulously monitored using GC MS (see SI†, Figure S1). Alongside the formation of diols **4** ($m/z = 184$, **C3**; see SI†, Figure S1), byproducts such as partially reduced compounds ($m/z = 182$; **C2**, Figure S1) and unreacted dialdehydes **3** were also detected ($m/z = 180$, **C1**; see SI†, Figure S1). Additionally, light-boiling byproducts from the hydroformylation step remained in the reaction mixture (**A** and **B**; see SI†, Figure S1). The desired products **4** were successfully isolated after full conversion of **3** with yields ranging from 45% to 67%, based on ENB (**1**), using vacuum distillation. For comparison, the patent procedure using dicyclopentadiene (DCPD) achieved a 71% yield of TCD-DM.⁴⁰ Prolonged reaction

times exceeding 14

View Article Online

DOI: 10.1039/D5PY00247H

Table 1. Hydrogenation of a crude product mixture of dialdehydes **3** using Raney nickel as the catalyst in toluene/H₂O solution (o.n. = over night: > 16 h), n.d. = not determined when full conversion of **3** was not completed; reaction conditions: 24.96 mmol **3**, 2 wt% Raney nickel, 10 wt% H₂O, 50 bar H₂.

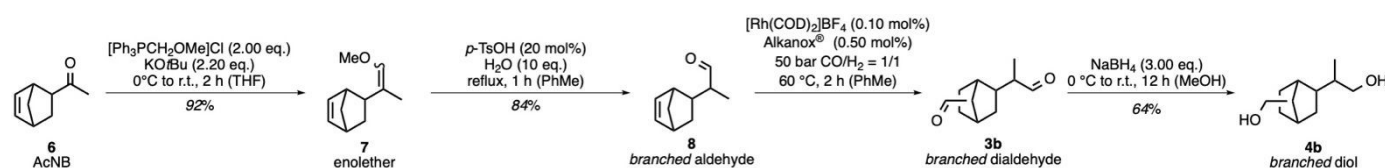
#	T [°C]	H ₂ usage [bar]	time [h]	yield [%]	full conversion of 3
1	r.t.	5.0	o.n.	n.d.	no
2	40	6.0	o.n.	45	yes
3	60	7.5	o.n.	n.d.	no
4	80	9.0	o.n.	66	yes
5	100	10	o.n.	66	yes
6	120	9.0	14	n.d.	no
7	140	10	4.5	67	yes

hours were noted at temperatures below 140 °C. However, at 140 °C, hydrogenation was completed within five hours. Trace amounts of the Rh-catalyst could interfere with conversion rates and hinder product isolation during vacuum distillation. Consequently, strategy (b) was employed for the reduction of purified dialdehydes **3**, leading to improved yields. The initial scale-up was conducted at 171 mmol scale at 140 °C, with optimized conditions using 4 wt% Raney nickel and 20 wt% H₂O, yielding 82% diols **4** (Scheme 3).

Simultaneously, the hydrogenation of linear dialdehydes **3c** was conducted on the crude product mixture at reaction temperatures of 80 °C and 100 °C. The resulting yields ranged from 16% to 31%, which are considerably lower compared to the hydrogenation of dialdehydes **3**. In both cases, the catalyst concentration was maintained at 2 wt% Raney nickel with 10 wt% H₂O. To achieve complete conversion of linear dialdehydes **3c** while preventing undesired side reactions, temperatures of at least 80 °C were deemed sufficient. Based on the previously optimized hydrogenation conditions of **3** using 4 wt% Raney nickel and 20 wt% H₂O, the hydrogenation process was successfully implemented on a 155 mmol scale. Hydrogenation of purified **3c** at 90 °C resulted in a 60% yield of linear diols **4c** (Scheme 3).

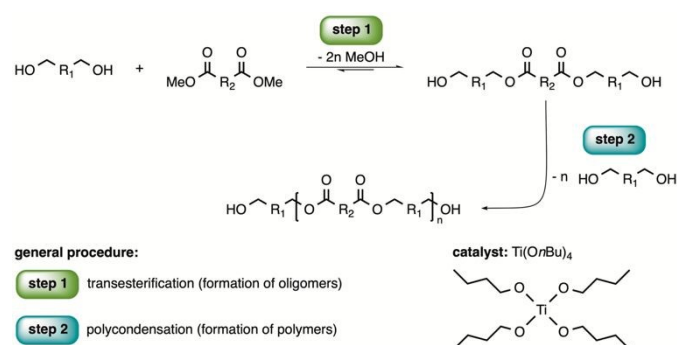
Proof of concept synthesis of branched diols **4b**

The targeted synthesis of linear diols **4c** suggests the possibility of selectively synthesizing branched dialdehydes. This approach may aid in screening structural dependencies on the thermal properties of polyesters. Building on the observed differences in the nature of the *endo*- and *exocyclic* double bonds of ENB (**1**) and VNB (**2**) during hydroformylation conditions, an alternative route towards branched diols **4b** was investigated (Scheme 4).⁴¹ Therefore, the branched moiety in **3b** was designed in two steps via Wittig reaction, followed by hydrolysis. The substrate



Scheme 4. Synthesis of branched dialdehydes **3b** via Rh-catalysed hydroformylation with Alkanox[®] as ligand, followed by reduction to the corresponding branched diols **4b**.





Scheme 5. General polycondensation procedure for the polyester synthesis (R_1/R_2 : alkyl).

5-acetyl-2-norbornene (AcNB, **6**) was converted with *in situ* generated phosphorus ylide (methoxymethylene)triphenyl phosphane to *cis/trans* enoether **7** in 92% yield. The hydrolysis to the corresponding *branched* aldehyde **8** was performed with 20 mol% *p*-toluenesulfonic acid monohydrate to yield 84%. These two transformations laid the foundation for the *branched* moiety in **4b**. Hence, the *endocyclic* double bond in **8** was implemented with the Rh-catalysed hydroformylation using Alkanox[®] as ligand. The crude product **3b** was initially reduced with NaBH_4 and MeOH to the corresponding *branched* diols **4b**. After purification with silica gel column chromatography, compound **4b** was isolated in 64% yield. The alternative route towards *branched* diols **4b** might not provide industrial scalability, but it allowed the access to *branched* isomers. Hence, the three diols **4**, **4b**, and **4c** possess structural differences and could show an intriguing influence on thermal properties in polyester synthesis.

Synthesis of amorphous polyesters and thermal structure-property relationships

To investigate the impact of *branched* and *linear* moieties on polyester microstructure, diols **4**, **4b**, and **4c** were synthesized and incorporated into polyesters via a two-step melt polycondensation reaction using dimethyl terephthalate (DMT) as a model compound. Titanium tetra-*n*-butoxide [$\text{Ti}(\text{OnBu})_4$, 0.20 mol%] was employed as catalyst (Scheme 5) to facilitate polymerization and enable a comparative study of structural influence on material properties. DMT was selected for its well-characterized thermal properties, allowing direct comparison with commercially relevant poly(ethylene terephthalate)s. Additionally, this method accommodates bio-based diacids of diesters such as dimethyl furan dicarboxylate (DMFD).

While purified terephthalic acid (TPA) is the predominant monomer in PET production, its use in laboratory-scale synthesis poses challenges due to the presence of residual

carboxylic acid groups, which can lead to side reactions, hinder chain growth, and potentially worsen alcoholysis. These issues are especially pronounced with thermally sensitive diols, such as 1,4-butanediol, which may undergo dehydration to tetrahydrofuran (THF) under esterification conditions.

In the transesterification step, a diol-to-diester mixture (2:1 molar ratio) was heated to 160 °C under ambient pressure, initiating methanol evolution. The temperature was incrementally increased by 10 °C to 220 °C until methanol evolution ceased (~5 to 6 hours), forming oligomeric precursor esters (Step 1, Scheme 5). Subsequently, under reduced pressure (0.05 mbar), the oligomeric mixture was heated to 240 °C for 2-3 hours to remove volatilized diols via distillation (Step 2, Scheme 5). The resulting amber-coloured polymer melt was dissolved in dichloromethane, precipitated, washed with cold methanol, and dried overnight at 70 °C under vacuum, yielding colourless to pale yellow polyesters (**P4T**, **P4bT**, and **P4cT**).

Polymerization with diols **4** produced medium- to high-molecular weight polymers ($M_{n,\text{rel}} = 7.89\text{--}19.2 \text{ kg mol}^{-1}$) with moderate to broad dispersities ($\bar{D} = 1.65\text{--}4.74$) (**P4T1-4**; see SI†, Table S2). While reaction conditions such as temperature, catalyst loading, and time were kept constant, the observed differences in molecular weight and dispersity across the **P4T1-4** series are attributed to variations in reaction scale. Initial reactions were performed on a smaller scale to assess monomer reactivity, followed by larger-scale polymerizations to obtain sufficient material for characterization. These scale differences likely influenced mixing efficiency and substrate dispersion, affecting polymer chain growth. Consistently, diols **4b** generated similar molecular weight distributions ($M_{n,\text{rel}} = 9.39\text{--}23.8 \text{ kg mol}^{-1}$) but with narrower dispersities ($\bar{D} = 2.10\text{--}2.70$) (**P4bT1-4**; see SI†, Table S2). However, the highest molecular weights in the **P4T** and **P4bT** series were obtained with $M_{n,\text{rel}} = 19.2 \text{ kg mol}^{-1}$ $M_{n,\text{rel}} = 23.8 \text{ kg mol}^{-1}$. The polymer containing *linear* diols **4c** exhibited a high molecular weight ($M_{n,\text{rel}} = 12.8 \text{ kg mol}^{-1}$) with a broad dispersity ($\bar{D} = 4.48$) (Table 2).

Achieving high-molecular-weight polymers requires precise end group-stoichiometry and efficient condensate removal to drive the reaction equilibrium toward polymer formation. The observed constraints in molecular weights and broad dispersities are characteristic of polycondensation due to inherent challenges, including:

- The necessity for exact stoichiometric balance between diester and diol, as minor deviations significantly reduce achievable molecular weights.
- Potential alcohol elimination during heating, leading to unreactive chain ends. Gas chromatography (GC) analysis detected volatile alcoholysis byproducts from excess diols removed during polymerization.

Table 2. Polycondensation of diols **4**, **4b** and **4c** with DMT (diol-to-diester ratio 2:1) at 220–240 °C yielding the respective polyesters **P4T**, **P4bT** and **P4cT**.

polyester	$M_{n,\text{rel}}^a [\text{kg mol}^{-1}]$	$M_{w,\text{rel}}^a [\text{kg mol}^{-1}]$	$\bar{D}^a [-]$	$T_d^b [^\circ\text{C}]$	$T_g^c [^\circ\text{C}]$
P4T	19.2	60.8	3.17	364	100
P4bT	23.8	63.3	2.70	379	103
P4cT	12.8	57.3	4.48	371	75



^aRelative molecular weight and dispersity measured via GPC in THF at 30 °C (25 mmol L⁻¹) relative to polystyrene. ^bOnset decomposition temperatures (T_d) of first decomposition step determined via TGA measurements. ^c T_g determined via DSC measurements. DOI: 10.1039/D5PY00247H

For industrial scalability, solid-state polymerization (SSP) can enhance molecular weight; however, its applicability is typically limited to semicrystalline polymers and may therefore be restricted for the predominantly amorphous polyesters described in this work.⁴²⁻⁴⁴

Understanding the thermal behaviour of these polyesters is essential for evaluating their potential high-temperature applications. Thermogravimetric analysis (TGA) and differential scanning calorimetry (DSC) were used to assess decomposition temperatures (T_d) and glass transition temperatures (T_g), revealing strong correlations with polymer chain length and structural differences.

TGA revealed T_d values between 361–381 °C for the P4T series, while P4bT and P4cT demonstrated slightly higher T_d values up to 387 °C (see SI†, Table S2). While this trend reflects general increases in molecular weight, it also highlights the influence of chain uniformity. Notably, the P4bT series displayed narrower molecular weight distributions and more consistent TGA profiles than P4T, suggesting that structural uniformity contributes to thermal stability. The broader variability observed in P4T may stem from the mixed regioisomer content of diol **4**, which could lead to microstructural deviations or sequence blockiness, depending on differences in reactivity and volatility among the isomers. These factors warrant further investigations, particularly with purified diol isomers to assess their impact on polymer architecture and thermal behaviour.

DSC analysis further highlighted the relationship between molecular weight and T_g . The T_g of P4T increased progressively with molecular weight, reaching 100 °C at $M_{n,rel} = 19.2$ kg mol⁻¹. The incorporation of *branched* moieties in P4bT resulted in higher T_g values reaching 103 °C at $M_{n,rel} = 23.8$ kg mol⁻¹, whereas the *linear* diols **4c** in P4cT notably reduced T_g to 75 °C at $M_{n,rel} = 12.8$ kg mol⁻¹. The lower T_g of P4cT is consistent with its lower molecular weight and the presence of flexible *linear* alkyl side chains, both which contribute to increased segmental mobility. Although the *linear* structure could facilitate tighter chain packaging, DSC analysis did not reveal any evidence of crystallinity (see SI†, Figure S28). Compared to previously reported biobased polyesters, none were found to combine M_n above 20.0 kg mol⁻¹ and T_g above 100 °C, highlighting the favourable thermal properties of P4bT.^{12, 20, 28, 45-51} Although direct comparison with commercial polyesters such as Tritan™ and PETG is premature due to differences in molecular weight and processing history, the reported T_g values (up to 103 °C) and thermal stability (T_d up to 387 °C) of the synthesized polyesters indicate promising potential for future development toward high-performance applications.

Incorporation of isosorbide in copolyesters: synthesis, characterization and thermal properties

The incorporation of isosorbide (IS, **9**; Figure 3) as a renewable diol in polyesters has been widely studied due to its ability to significantly increase T_g while enhancing optical properties, including improved transmittance and reduced haze.¹⁴ Additionally, dimethyl furan dicarboxylate (DMFD, **10**; Figure 3) is emerging as a promising alternative to DMT in polyester production. Literature reports indicate that polyesters synthesized with DMFD exhibit thermal and barrier properties comparable to petroleum-based poly(ethylene terephthalate)s (PET), making them attractive for sustainable polymer development.^{11, 45, 52-53}

In this study, a series of copolyesters – P4colST, P4ccolST, and P4colSF – were synthesized using a well-established two-step melt polycondensation process. These copolyesters incorporated diols **4**, *linear* diols **4c**, and isosorbide (IS), with DMT (T) and DMFD (F) serving as the corresponding diesters. The reaction was conducted using a diol-to-diacid molar ratio of 2:1. The chemical structure of the resulting copolyesters were characterized using ¹H NMR and DOSY NMR spectroscopy, while their thermal properties were evaluated using TGA and DSC. These properties were then compared to those of reference polyester P4T and P4cT. Although diols **4b** demonstrated superior molecular control over molecular weight and dispersity, along with high T_g values, it was not included in the copolymerization due to the increased synthetic effort required for its preparation. The more scalable synthesis of diols **4** and **4c** made them more suitable for evaluating industrially relevant systems.

The incorporation of IS into copolyesters P4colST, P4ccolST, and P4colSF presented specific challenges. Among these, P4colST exhibited the lowest molecular weight with a narrow dispersity (Table 3). The ¹H NMR analysis confirmed the presence of characteristic resonances for DMT and ester groups (-CH₂O-) of diols **4** and **4c**, similar to those observed in polyester P4T and P4cT. The aliphatic proton resonances of IS were identified between $\delta_{1H} = 5.51$ and 4.00 ppm, with chain end groups appearing at $\delta_{1H} = 5.00$ and 3.60 ppm. Aliphatic protons of DMFD were detected at $\delta_{1H} = 4.20$ ppm and $\delta_{1H} = 1.10$ ppm, respectively. By comparing the intensity peaks of aromatic protons in DMT and DMFD to those of the ester groups (-CH₂O-) of diols **4** and **4c**, the final molar ratios of IS in the copolyester were determined (Table 3). DOSY NMR spectroscopy further confirmed successful copolymerization, as the diffusion coefficients of proton signals from DMT and DMFD were identical to those of the respective diols (see SI†, Figure S14, S16 and S18).

Table 3. Polycondensation of diols **4**, **4b** and **4c** with IS and DMT / DMFD (diol-to-diester ratio 2:1) at 220–240 °C yielding the respective copolyesters P4colST, P4ccolST and P4colSF.

copolyester	mole fraction of IS in copolyester ^a [mol%]	$M_{n,rel}$ ^b [kg mol ⁻¹]	$M_{w,rel}$ ^b [kg mol ⁻¹]	\bar{D}^b [–]	T_d ^c [°C]	T_g ^d [°C]
P4colST	5.00	7.37	12.9	1.76	373	97
P4ccolST	1.50	17.3	38.5	2.07	363	81
P4colSF	2.50	13.4	31.9	1.88	340	89



^aMole fraction of IS in copolyester, determined by integration in ¹H NMR spectra. ^bRelative molecular weight and dispersity measured via GPC in THF at 30 °C (25 mol% IS). ^cRelative to polystyrene. ^dOnset decomposition temperatures (*T_d*) of first decomposition step determined via TGA measurements. ^e*T_g* determined via DSC measurements.

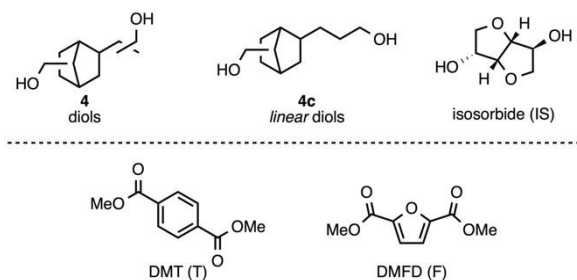


Figure 3. Depicted diol and diester monomers for the synthesis of copolyester **P4colST**, **P4ccolST** and **P4colSF**.

Achieving high transesterification conversion, which facilitates polycondensation, requires efficient removal of alcohol byproducts to drive the reaction equilibrium. However, IS negatively impacted the polycondensation process, reducing the conversion rate and yielding shorter oligomers. Additionally, co-diols with lower boiling points than isosorbide reacted more quickly and evaporated more readily, further complicating the reaction.^{14, 54}

Despite these challenges, the transesterification step remained unaffected, with methanol evolution completing within 5–6 hours. However, the polycondensation step was more complex, relying on rapid alcoholysis and efficient elimination of terminal diols under high vacuum (< 1 mbar). The boiling points of IS¹⁴ and diols **4** overlapped (105–120 °C vs. 120 °C, respectively), complicating selective removal. Linear diols **4c** exhibited a slightly higher boiling point (130 °C), which influenced their behaviour in polycondensation. Our findings align with previous studies by Fenouillot *et al.*, who investigated the reactivity of IS. They found that primary bicyclic diols, such as diols **4** and **4c**, can induce steric hindrance, whereas the secondary bicyclic structure of IS allows for better accessibility to ester groups.¹⁴ Furthermore, the hydrophobic nature of diols **4** and **4c** contrast with the hydrophilic properties of IS, making hydrophilic ester bond formation more challenging when diols **4b** or **4c** are present at both chain ends.¹⁴ Fenouillot's study also suggested that IS can act as a promoter, accelerating the polycondensation step.¹⁴

Comparing the molecular weights of **P4colST** ($M_{n,rel} = 7.37 \text{ kg mol}^{-1}$) and **P4ccolST** ($M_{n,rel} = 17.3 \text{ kg mol}^{-1}$), it was evident that copolymerization of IS with linear diols **4c** resulted in higher molecular weights. This suggests that IS acted more effectively as a “chain linker” than linear diols **4c**, leading to lower IS content (1.50 mol%) in **P4ccolST**. In contrast, the copolymerization of IS with diols **4** proved more complex, likely due to a mixture of sterically hindered isomers (branched vs. linear). The overlapping boiling points further complicated the removal process, leading to higher IS content in **P4colST** (5.00 mol%) compared to **P4ccolST** (1.50 mol%). These observations suggest that future studies should explore separating regioisomers **4a**, **4b**, and **4c** as model compounds to

better understand reactivity differences between hydrophobic diols and hydrophilic IS.

Despite precipitation and methanol washing, **P4colSF** (2.50 mol% IS content) exhibited a pale-yellow colour, a common issue associated with high polymerization temperatures.^{11, 45, 53} Although DMFD was used to mitigate decarboxylation, prolonged reaction times (> 16 hours) and high melt viscosity hindered heat and mass transfer. However, replacing DMT with DMFD provides significant advantages, including improved crystallization behaviour, ensuring amorphous morphologies suitable for industrial processing. Additionally, poly(ethylene 2,5-furandicarboxylate) polyesters exhibit significantly lower gas permeabilities (O₂, CO₂, and H₂O) due to reduced chain mobility, making them promising candidates for food packaging applications.¹¹

Thermal analysis using TGA and DSC revealed distinct structure-property relationships in copolyesters incorporating IS (Table 3). **P4colST** and **P4ccolST** demonstrated high thermal stability, with *T_d*s of 373 °C and 363 °C, comparable to *T_d* = 363–379 °C (see S1†, Table S2) observed in reference polyesters **P4T** and **P4cT**. In contrast, **P4colSF** exhibited a lower *T_d* of 340 °C. Despite this, all copolyesters displayed excellent thermal stability, making suitable for high-temperature applications such as injection molding. DSC analysis highlighted the influence of molecular weight on *T_g*. The *T_g* of **P4colST** (97 °C) was significantly higher than that of **P4T1** (87 °C; see S1†, Table S2) despite similar molecular weights, aligning with previous studies that 6 mol% IS can increase *T_g* by 10 °C.¹⁸ Conversely, the incorporation of 2.50 mol% IS in **P4colSF** did not significantly affect *T_g*, which remained at 89 °C, compared to 92 °C for the polyester **P4T2** (see S1†, Table S2). In contrast, in the copolyester **P4ccolST**, 1.50 mol% IS content increased *T_g* to 81 °C, compared to 75 °C in **P4cT**. This suggests that even low IS content can have a noticeable influence on thermal properties, particularly in systems incorporating linear diols. Additionally, the variation in *T_g* between different copolyesters highlights the importance of precise monomer selection and polymerization conditions to achieve desired thermal characteristic.

Further investigation into the molecular dynamics of these copolyesters could provide deeper insights into the structural effects of IS incorporation. Future studies could explore the interplay between chain rigidity, segmental mobility, and hydrogen bonding interactions to fully understand the role of rigid cyclic diols in polyester performance. Moreover, optimizing reaction conditions to further increase molecular weight while maintaining favourable thermal properties will be crucial for advancing these materials in industrial applications such as sustainable packaging and coatings.

Conclusions

This study highlights the potential of utilizing alicyclic-diene-based polyols as key components for synthesizing amorphous, high *T_g* polyesters. The successful



synthesis and scale-up of dialdehydes **3** and **3c** were achieved through optimized hydroformylation reactions using two regio-directing ligands. The subsequent hydrogenation process to produce diols **4** and linear diols **4c** was effectively carried out using Raney nickel, a widely used industrial heterogeneous catalyst. Despite these advancements, further improvements in purification methods are necessary to maximize the yields of reactive dialdehydes.

Additionally, an alternative pathway for synthesizing branched diols **4b** was established, allowing for an investigation into influence of different regio- and diastereomers on polyester properties. The synthesized diols **4**, **4b** and **4c** provided a platform for developing amorphous polyesters with medium-to-high molecular weights. While complete molecular weight optimization was not achieved, the resulting polyesters exhibit promising thermal properties, with T_g values ≥ 100 °C.

Although the synthesis of monomers **4** and **4c** still relies on petroleum-based raw materials, this work advances the development of partially biobased polyesters by incorporating sustainable building blocks such as IS and DMFD. Notably, the incorporation of 5.00 mol% IS in P4colST-type copolyester significantly increased the glass transition temperature ($T_g = 97$ °C), despite low molecular weight ($M_{n,rel} = 7.37$ kg mol⁻¹). Similarly, in P4ccolST-type copolyester, IS incorporation increased T_g from 75 °C to 81 °C. The replacement of DMT with DMFD presents additional advantages in terms of mechanical and barrier properties. Although P4colSF copolyester exhibited promising thermal properties, achieving higher molecular weight ($M_n > 20$ kg mol⁻¹) will be essential for optimizing mechanical performance.

Cycloaliphatic structures offer significant advantages not only in polyesters but also in poly(amide)s (PA)⁵⁴, poly(urethane)s (PU)⁵⁵ or poly(methyl methacrylate)s (PMMA)⁵⁶. Incorporating cycloaliphatic moieties into these polymers enhances their properties, making them more suitable for demanding applications that require enhanced UV stability, mechanical strength, and thermal resistance. These enhanced properties enable their use in a wide range of applications, including automotive parts, optical components, coatings, adhesives, and consumer goods.

The polymer precursors developed in this study open new avenues for synthesizing novel monomers, including amines, carboxylic acids, and methyl methacrylates. These advancements will facilitate the development of innovative copolymers tailored to meet the stringent requirements of high-performance applications, extending both the usability and lifespan of advanced materials.

Author contributions

Brigita Bratić: conceptualization, synthesis, funding acquisition, writing original draft, visualization, data curation, formal analysis; Peter Altenbuchner: writing – review & editing, visualization, data curation, formal analysis; Thomas Heuser: writing – review & editing, visualization, data curation, formal analysis; Bernhard Rieger: funding acquisition, supervision, project administration, resources, writing – review & editing.

Conflicts of interest

There are no conflicts to declare.

Data availability

The data supporting this article have been included as part of the Supplementary Information.

Acknowledgements

The authors want to thank Dr. Fabian Martin Hörmann and Stefanie Hörl for the great proofreading process. Additionally, the authors are grateful for the good discussion with the group of the WACKER Chair of Macromolecular Chemistry and Evonik Industries. The authors additionally want to thank Evonik Industries for support and funding.

References

- 1 R. Hatti-Kaul, L. J. Nilsson, B. Zhang, N. Rehnberg, S. Lundmark, *Trends Biotechnol.* **2019**, *38*, 1-67.
- 2 R. Mori, *RSC Sustainability* **2023**, *1*, 179-212.
- 3 M. Zhang, G. M. Biesold, W. Choi, J. Yu, Y. Deng, C. Silvestre, Z. Lin, *Mater. Today* **2022**, *53*, 134-161.
- 4 V. T. Weligama Thuppahige, M. A. Karim, *Compr. Rev. Food Sci. Food Saf.* **2022**, *21*, 689-718.
- 5 C. Lambré, J. M. Barat Baviera, C. Bolognesi, A. Chesson, P. S. Cocconcelli, R. Crebelli, D. M. Gott, K. Grob, E. Lampi, M. Mengelers, A. Mortensen, G. Riviére, V. Silano, I. L. Steffensen, C. Tlustos, L. Vernis, H. Zorn, M. Batke, M. Bignami, E. Corsini, R. Fitzgerald, U. Gundert-Remy, T. Halldorsson, A. Hart, E. Ntzani, E. Scanziani, H. Schroeder, B. Ulbrich, D. Waalkens-Berendsen, D. Woelfle, Z. Al Harraq, K. Baert, M. Carfi, A. F. Castoldi, C. Croera, H. Van Loveren, *EFSA J.* **2023**, *21*, e06857.
- 6 J. S. Siracusa, L. Yin, E. Measel, S. Liang, X. Yu, *Reprod. Toxicol.* **2018**, *79*, 96-123.
- 7 A. Abraham, P. Chakraborty, *Rev. Environ. Health* **2019**, *2*, 201-210.
- 8 Y. B. Wetherill, B. T. Akingbemi, J. Kanno, J. A. McLachlan, A. Nadal, C. Sonnenschein, C. S. Watson, R. T. Zoeller, S. M. Belcher, *Reprod. Toxicol.* **2007**, *24*, 178-198.
- 9 S. Mangaraj, A. Yadav, L. M. Bal, S. K. Dash, N. K. Mahanti, *J. Packag. Technol. Res.* **2019**, *3*, 77-96.
- 10 F. Fenouillot, A. Rousseau, G. Colomines, R. Saint-Loup, J.-P. Pascault, *Prog. Polym. Sci.* **2010**, *35*, 578-622.
- 11 D. Zhang, M. J. Dumont, *J. Polym. Sci. Part A: Polym. Chem.* **2017**, *55*, 1478-1492.
- 12 J. Wang, X. Liu, Z. Jia, Y. Liu, L. Sun, J. Zhu, *J. Polym. Sci. Part A: Polym. Chem.* **2017**, *55*, 3298-3307.
- 13 M. N. S. Kumar, Z. Yaakob, Siddaramaiah, in *Handbook of Bioplastics and Biocomposites Engineering Applications* (Ed.: S. Pilla), **2011**, pp. 121-160.
- 14 S. Legrand, N. Jacquél, H. Amedro, R. Saint-Loup, M. Colella, J.-P. Pascault, F. Fenouillot, A. Rousseau, *ACS Sustainable Chem. Eng.* **2020**, *8*, 15199-15208.
- 15 J. Thiem, H. Lüders, *Polym. Bull.* **1984**, *11*, 365-369.
- 16 R. Storbeck, M. Rehahn, M. Ballauff, *Makromol. Chem.* **1993**, *194*, 53-64.
- 17 R. Storbeck, M. Ballauff, *J. Appl. Polym. Sci.* **1996**, *59*, 1199-1202.



- 18 H. R. Kricheldorf, G. Behnken, M. Sell, *J. Macromol. Sci., Part A: Pure Appl. Chem.* **2007**, *44*, 679-684.
- 19 R. Storbeck, M. Ballauff, *Polymer* **1993**, *34*, 5003-5006.
- 20 W. J. Yoon, S. Y. Hwang, J. M. Koo, Y. J. Lee, S. U. Lee, S. S. Im, *Macromolecules* **2013**, *46*, 7219-7231.
- 21 T. Kim, J. M. Koo, M. H. Ryu, H. Jeon, S.-M. Kim, S.-A. Park, D. X. Oh, J. Park, S. Y. Hwang, *Polymer* **2017**, *132*, 122-132.
- 22 S. Legrand, N. Jacquél, H. Amedro, R. Saint-Loup, J.-P. Pascault, A. Rousseau, F. Fenouillot, *Eur. Polym. J.* **2019**, *115*, 22-29.
- 23 S. R. Turner, *J. Polym. Sci. Part A: Polym. Chem.* **2004**, *42*, 5847-5852.
- 24 R. Quintana, A. M. De Ilarduya, A. Alla, S. Muñoz-Guerra, *J. Polym. Sci. A: Polym. Chem.* **2011**, *49*, 2252-2260.
- 25 G. W. Baell, C. E. Powell, J. Hancock, M. Kindinger, H. R. McKenzie, A. V. Bray, C. J. Booth, *Appl. Clay Sci.* **2007**, *37*, 295-306.
- 26 M. Zhang, R. B. Moore, T. E. Long, *J. Polym. Sci. Part A: Polym. Chem.* **2012**, *50*, 3710-3718.
- 27 J. Wang, S. Mahmud, X. Zhang, J. Zhu, Z. Shen, X. Liu, *ACS Sustainable Chem. Eng.* **2019**, *7*, 6401-6411.
- 28 J. Wang, X. Q. Liu, Y. J. Zhang, F. Liu, J. Zhu, *Polymer* **2016**, *103*, 1-8.
- 29 S. Hong, K.-D. Min, B.-U. Nam, O. O. Park, *Green Chem.* **2016**, *18*, 5142-5150.
- 30 J. Wang, X. Q. Liu, Z. Jia, L. Sun, Y. J. Zhang, J. Zhu, *Polymer* **2018**, *137*, 173-185.
- 31 R. Franke, D. Selent, A. Börner, *Chem. Rev.* **2012**, *112*, 5675-5732.
- 32 Y. G. Osokin, *Pet. Chem.* **2007**, *47*, 1-11.
- 33 D. Mijolovic, V. Wendel, A. Suckert, BASF SE, WO 2011023540 A2, **2011**.
- 34 A. Bara-Estaun, C. Lyall, J. P. Lowe, P. G. Pringle, P. Kamer, R. Franke, U. Hintermair, *Faraday Discussions* **2020**.
- 35 C. Kubis, R. Ludwig, M. Sawall, K. Neymeyr, A. Börner, K.-D. Wiese, D. Hess, R. Franke, D. Selent, *Chem. Cat. Chem.* **2010**, *2*, 287-295.
- 36 G. M. Noonan, J. A. Fuentes, C. J. Cobley, M. L. Clarke, *Angew. Chem.* **2012**, *124*, 2527-2530.
- 37 P. Dingwall, J. A. Fuentes, L. E. Crawford, A. M. Z. Slawin, M. Bühl, M. L. Clarke, *J. Am. Chem. Soc.* **2017**, *139*, 15921-15932.
- 38 D. Selent, R. Franke, C. Kubis, A. Spannenberg, W. Baumann, B. Kreidler, A. Börner, *Organometallics* **2011**, *30*, 4509-4514.
- 39 B. Kreidler, D. Fridag, B. Schemmer, B. Wechsler, A. Christiansen, D. Neumann, *Evonik Oxeno GmbH*, DE 10 2011 002 639 A1, **2011**.
- 40 W. Dukat, E. Storm, K. Schmid, *Oxea Deutschland GmbH*, US 7301057 B2, **2005**.
- 41 P. A. Byrne, D. G. Gilheany, *Chem. Soc. Rev.* **2013**, *42*, 6670-6696.
- 42 S.N. Vouyiouka, E.K. Karakatsani, C. D. Papaspyrides, *Progr. Polym. Sci.* **2005**, *30*, 10-37.
- 43 F. C. Chen, R. G. Griskey, G. H. Beyer, *AIChE J.* **1969**, *15*, 680-685.
- 44 K. D. Samant, K. M. Ng, *AIChE J.* **1999**, *45*, 1808-1829.
- 45 R. J. I. Knoop, W. Vogelzang, J. Van Haveren, D. S. Van Es, *J. Polym. Sci. Part A: Polym. Chem.* **2013**, *51*, 4191-4199.
- 46 J. G. Wang, X. Q. Liu, J. Zhu, Y. Jiang, *Polymers* **2017**, *9*, 305.
- 47 J. G. Van Berkel, N. Guigo, J. J. Kolstad, L. Sipos, B. Wang, M. A. Dam, N. Sbirrazzuoli, *Macromol. Mater. Eng.* **2015**, *300*, 466-474.
- 48 M. Jiang, Q. Liu, Q. Zhang, C. Ye, G. Zhou, *J. Polym. Sci. Part A: Polym. Chem.* **2012**, *50*, 1026-1036.
- 49 M. Vannini, P. Marchese, A. Celli, C. Lorenzetti, *Green Chem.* **2015**, *17*, 4162-4166.
- 50 G. Z. Papageorgiou, D. G. Papageorgiou, Z. Terzopoulou, D. N. Bikiaris, *Eur. Polym. J.* **2016**, *83*, 202-229.
- 51 M. Garaleh, T. Yashiro, H. R. Kricheldorf, P. Simon, S. Chatti, *Macromol. Chem. Phys.* **2010**, *211*, 1206-1214.
- 52 J. Carlos Morales-Huerta, A. Martínez De Ilarduya, S. Muñoz-Guerra, *Polymer* **2016**, *87*, 148-158.
- 53 W. H. Carothers, *Trans. Faraday Soc.* **1936**, *32*, 39-49.
- 54 C.-W. Chen, C.-W. Lin, Y.-H. Chen, T.-F. Wei, S.-P. Rwei, R. Sasikumar, *Polym. Bull.* **2020**, *77*, 235-253.
- 55 A. Mouren, L. Avérous, *Chem. Soc. Rev.* **2023**, *52*, 277-317.
- 56 S. K. Asha, V. Deepthimol, M. Lekshmi, *J. Polym. Sci. Part A: Polym. Chem.* **2004**, *42*, 5617-5626.



View Article Online
DOI: 10.1039/D5PY00247H

Data availability

The data supporting this article have been included as part of the Supplementary Information.

